

# Influences of sintering process on (Bi<sub>2</sub>O<sub>3</sub>–V<sub>2</sub>O<sub>5</sub>–Mn<sub>3</sub>O<sub>4</sub>–Y<sub>2</sub>O<sub>3</sub>–Co<sub>2</sub>O<sub>3</sub>–Cr<sub>2</sub>O<sub>3</sub>)-doped ZnO varistors

Jianke Liu<sup>1</sup>  · Yongjia Chen<sup>2</sup> · Yonghong Cui<sup>1</sup> · Chen Han<sup>2</sup> · Cheng Zhang<sup>1</sup> · Yahong Fan<sup>1</sup> · Chuxuan Liang<sup>1</sup>

Received: 11 July 2016 / Accepted: 30 September 2016 / Published online: 6 October 2016  
© Springer Science+Business Media New York 2016

**Abstract** The effects of sintering temperatures on the microstructure, electrical and dielectric properties of (V<sub>2</sub>O<sub>5</sub>–Bi<sub>2</sub>O<sub>3</sub>–Mn<sub>3</sub>O<sub>4</sub>–Y<sub>2</sub>O<sub>3</sub>–Cr<sub>2</sub>O<sub>3</sub>–Co<sub>2</sub>O<sub>3</sub>)-doped ZnO varistors had been researched systematically. The results showed that, when the sintering temperature increased from 870 to 930 °C, the following changes occurred: the average grain size enlarged from 0.83 to 1.67 μm and the density increased from 4.97 to 5.3 g/cm<sup>3</sup>. The conclusion can be drawn that the optimal microstructure and uniformity could be obtained at 910 °C; Meanwhile, it was observed that the breakdown electrical field  $E_{1mA}$  decreased from 5127.3 to 2687.5 V/cm and the nonlinear coefficient  $\alpha$  was likely to increase as the sintering temperature increased, however, the latter decreased to 15.6 sharply at 930 °C; Simultaneously, it was noted that the relative dielectric constant  $\epsilon_r$  and the dielectric loss  $\tan\delta$  increased first and then decreased as the sintering temperature increasing when the frequency was 10 kHz. Another conclusion can be drawn that the best electrical and dielectric properties were obtained at 910 °C, where  $\alpha$  was 27,  $E_{1mA}$  was 3456.5 V/cm; when the frequency was 10 kHz the values of  $\epsilon_r$  and  $\tan\delta$  were 194 and 0.29 at this sintering temperature, respectively. Meanwhile, the temperature coefficient of resistance  $\alpha_T$  was only –0.67 % and the impedance was also fairly stable at this sintering temperature.

## 1 Introduction

The fast development of the power electronic technology gives rise to the era of microelectronic products, such as smart phone, ultra-thin TV, the miniature spy plane and military radar in military industry. However, their further miniaturization, intellectualization and integration have been affected by the surges. The surges, which are transient voltages or circuits occurring in a very short time, like several microseconds, have serious effects on the power electronic devices, and even can make some electronic equipments breakdown. Therefore, it is very necessary to absorb the surgy energy effectively in order to prevent the system from the destructions of over-voltages to a stable power electronic system. In recent years, the common core component of varistors is zinc oxide (ZnO), and these varistors are very stable to over-voltages. Generally, these varistors are composed of the zinc oxide grains as the main crystal phase and other oxide impurities around the zinc oxide grains as the boundary phases. A qualified ZnO varistor has much higher capability of surge handling and its voltage–current relation is similar to a back-to-back zener diode [1, 2].

The studies of ZnO–Bi<sub>2</sub>O<sub>3</sub>-based and ZnO–Pr<sub>6</sub>O<sub>11</sub>-based varistors showed that these systems can lead to essential nonlinear properties [2, 3]. At the same time, it is reported that some ZnO varistors were doped with Bi<sub>2</sub>O<sub>3</sub> instead of Pr<sub>6</sub>O<sub>11</sub> [3]. Besides, ZnO varistors can be made into a multilayer one, which is equivalent to putting several varistors in series. As a result, the performances and the service life could be obviously improved. However, the common sintering temperature of multilayer ZnO varistors is generally as high as 1000 °C [4, 5], so the ZnO varistors doped with bismuth cannot be sintered with pure silver as the material of inner-electrodes in the multilayer varistors

✉ Jianke Liu  
1208091455@qq.com

<sup>1</sup> College of Science, Shaanxi University of Science and Technology, Xi'an 710021, China

<sup>2</sup> College of Electrical and Information Engineering, Shaanxi University of Science and Technology, Xi'an 710021, China

and only some precious metals, such as Pt and Pd, can be used. Studies had shown that the sintering temperature of ZnO varistor doped with vanadium was low [6, 7], so the relatively cheap pure silver can be used as the material of inner-electrodes to reduce the costs. It was also reported that the low sintering temperature ZnO varistors had many outstanding performances [8–10]. Therefore, it was very necessary to study the effects of sintering system on the microstructure and electrical properties of ZnO varistors with specific composition [11–20]. In this paper, the effects of sintering temperature on microstructure and electrical properties of ( $V_2O_5$ – $Bi_2O_3$ – $Mn_3O_4$ – $Y_2O_3$ – $Cr_2O_3$ – $Co_2O_3$ )-doped ZnO varistors were systematically studied and some new results were obtained.

## 2 Experiments

The formulation had been prepared with analytical grade raw materials in the proportion of 95.5ZnO–0.5V<sub>2</sub>O<sub>5</sub>–2.0Bi<sub>2</sub>O<sub>3</sub>–0.5Mn<sub>3</sub>O<sub>4</sub>–0.5Y<sub>2</sub>O<sub>3</sub>–0.5Cr<sub>2</sub>O<sub>3</sub>–0.5Co<sub>2</sub>O<sub>3</sub> (mol%). The raw materials had been mixed with aluminium oxide balls and water in the planetary ball mill for 24 h with the rotation speed of 530 r/min, and the mass ratio of aluminium oxide balls to the material powders and water was 2:1:2. The mixture had been dried at 120 °C for 12 h, and the dried mixture had been grinded to powders again in a Al<sub>2</sub>O<sub>3</sub> mortar. Then, the powders had been prilled by mingling with 8.0 wt% polyvinyl alcohol (PVA), and the conglobate granules had been filtrated between the sifters of 80 and 120 meshes. Staled for 24 h, the chosen granules had been uniaxially pressed into discs of 10 mm in diameter and 1.5 mm in thickness approximately under the pressure of 500 MPa by the powder pressing machine. The pressed discs had been put in the Al<sub>2</sub>O<sub>3</sub> saggar, and removed binder at 550 °C for 4 h, then these discs had been sintered at 870, 890, 910, 930 °C respectively for 6 h, keeping the heating and falling rate at 3 °C/min. The sintered discs were about 8 mm in diameter and 1 mm in thickness approximately. Some of the sintered discs had been lapped and polished, then the pure silver paste had been coated on both faces of these polished discs. Heated at 600 °C for 10 min, the electrodes had been formed.

To characterize the microstructure, the surfaces of the sintered discs had been polished with SiC sandpapers of 400, 1000 and 2000 meshes. The surface microstructure would be shown by a scanning electron microscope (SEM, HITACH, FE-S4800, Japan) equipped with energy-dispersive spectroscopy (EDS). The average grain size would be calculated by the lineal intercept method [21]. The density of these sintered discs would be measured by the Archimedes method according to international standard (ISO18754). The crystal phases would be identified by the

X-ray diffraction (XRD, Model Rigaku-D/Max-2200PC, Japan) using Cu K<sub>α</sub> radiation.

The nonlinear coefficient  $\alpha$ , breakdown electrical field  $E_{1mA}$  and the electric field-current density ( $E$ – $J$ ) characteristics would be shown by a DC parametric equipment of varistors (CJ1001). The impedance, resistivity and dielectric properties would be measured by a high temperature dielectric measure system (GJM-I, EMRL XJTU).

## 3 Results and discussions

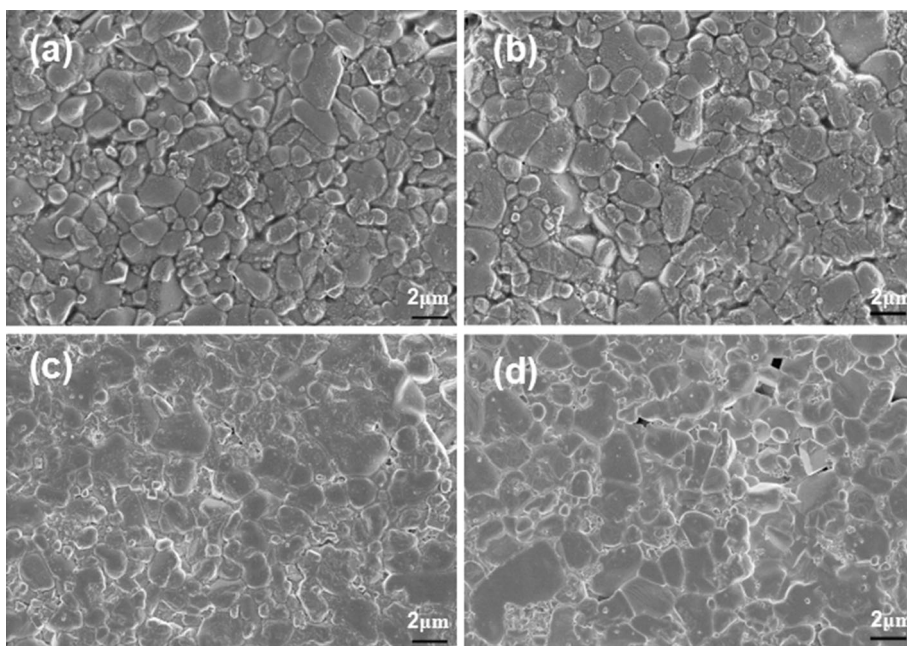
### 3.1 Analysis of microstructure

Figure 1 showed the SEM micrographs of ZnO varistors with different sintering temperatures. The average grain size increased from 0.83 to 1.67  $\mu$ m when the sintering temperature increased from 870 to 930 °C. On the whole, the average grain size of ZnO varistors increased and the contents of secondly main phases added as well.

Table 1 showed the characteristics of microstructure and electrical properties of ZnO varistors sintered in different temperatures. The EDS spectrum, which was shown in Fig. 2, explained the composition of the grain boundary phases, in which the octahedral particles may be spinel phases. When the ZnO ceramics were sintered at 910 and 930 °C, abundant spinel phases appeared. However, the reunion phenomenon occurred when the sintering temperature was 930 °C, which was likely to cause the abnormal growth of ZnO grains. This phenomenon was mainly attributed to the different sintering temperatures. The raw materials would go through the sintering process with four stages when the sintering temperature increased, which is the contraction of powders, the reactions of powders, the nucleation of ZnO grains and the growing of ZnO grains. As the sintering temperature was 930 °C, the sintering reactions had been going for a long time. Overmuch spinel phases were synthesized, so some of these phases were reunited in the grain boundaries at 930 °C.

Figure 3 showed the XRD results of ZnO varistors sintered in different temperatures. The main phase was hexagonal wurtzite ZnO (PDF:75-0576) [22–24]. At the same time, the BiVO<sub>4</sub>, YVO<sub>4</sub>, Zn<sub>2</sub>V<sub>2</sub>O<sub>7</sub>, Co<sub>3</sub>V<sub>2</sub>O<sub>8</sub> and CoCr<sub>2</sub>O<sub>4</sub> phases could be detected in the patterns to all the prepared varistors. However, little phases with the manganese element were observed. This agreed with the results reported by Choow-W Nahm [25], who studied the effect of ZVMCD varistor ceramics with manganese doping. Figure 4 showed the partially enlarged XRD patterns of all the prepared varistors with the diffraction angle 2-Theta between 30° and 40°. The diffraction peaks of the samples were moved to the low angle as the sintering temperature increasing. This may be attributed to the increase of the

**Fig. 1** SEM micrographs of ZnO varistors at different sintering temperatures. **a** 870 °C, **b** 890 °C, **c** 910 °C, **d** 930 °C

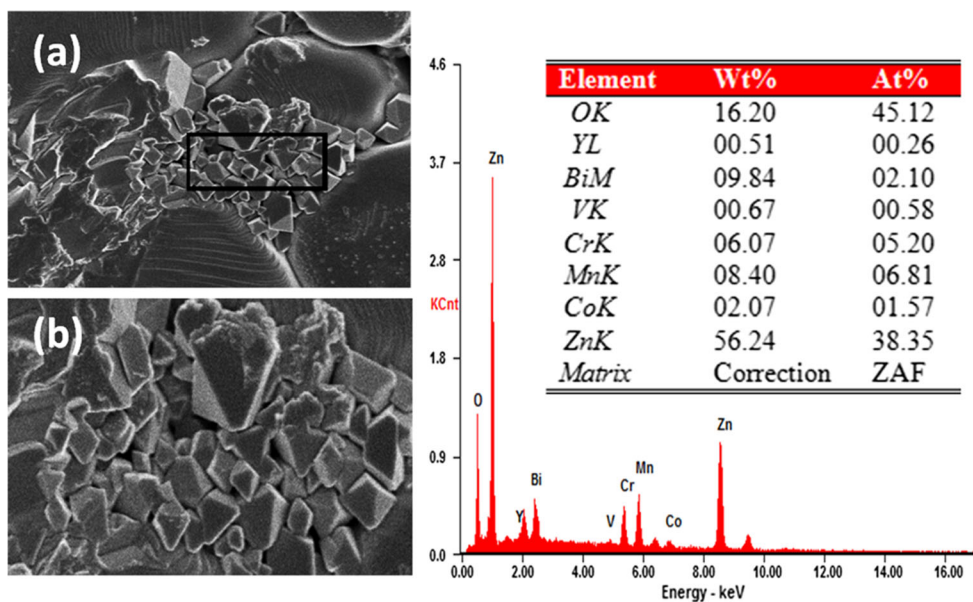


**Table 1**  $E$ - $J$ ,  $\alpha$  and structure parameters of the samples sintered in different temperatures

Sintering temperature (°C)	$E_{1mA}$ (V/cm)	$\alpha$	Average grain size ( $\mu\text{m}$ )	Volume shrinkage rate (%)	Relative density (%)
870	5127.3	19.1	0.83	17.83	88.67
890	4047.6	13.3	1.00	18.46	88.62
910	3456.5	27	1.25	19.53	94.26
930	2687.5	15.6	1.67	19.56	94.68

The density of ZnO is  $5.606 \text{ g cm}^{-3}$

**Fig. 2** SEM micrograph of **a** the varistor sintered at 910 °C and **b** its partial enlargement with EDS spectrum



crystal parameter  $a$  or  $c$  and the interplanar spacing  $d$  as the sintering temperature increasing. According to the bragg's law evaluated by the Eq. (1), in which  $d$  is the interplanar

spacing,  $\theta$  the half of the diffraction angle, and  $\lambda$  is the wavelength of the X-ray, this phenomenon could be explained.

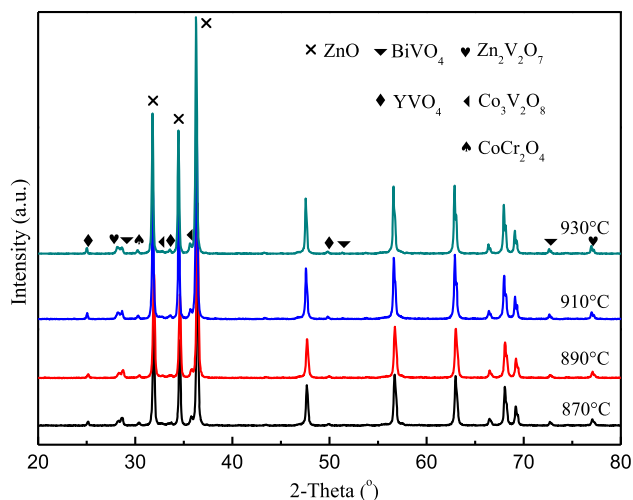


**Fig. 3** XRD patterns of the varistors with different sintering temperatures

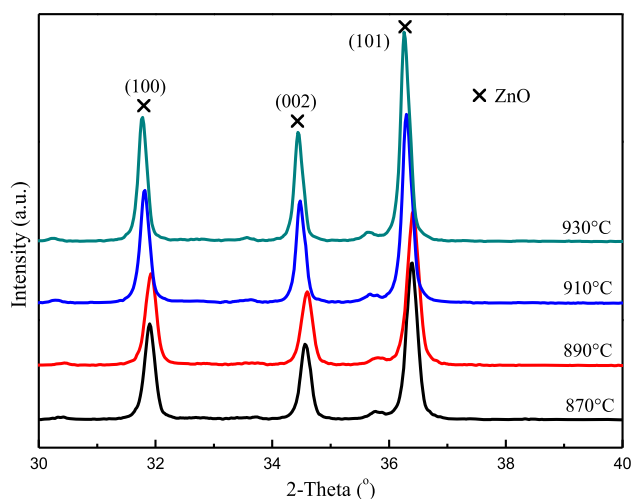


**Fig. 4** The partially enlarged XRD patterns with  $2\theta$  between  $30^\circ$  and  $40^\circ$

$$2d \sin \theta = \lambda \quad (1)$$

Figure 5 showed the lattice parameters  $a$  and  $c$  of the ZnO ceramics. The conclusion can be drawn that these measured values were similar to the theoretical values (The value of  $a$  is  $3.2568 \text{ \AA}$  and the value of  $c$  is  $5.2125 \text{ \AA}$ ). Meanwhile, the lattice parameters  $a$  and  $c$  were the maximum when the sintering temperature was  $930^\circ\text{C}$ , which was coincided with the results of XRD. The relative density and volume shrinkage rate of the varistors sintered in different temperatures were shown in Fig. 6. The results indicated that the volume shrinkage rate and the relative density were in an increasing tendency as the sintering temperature increasing. However, the relative density of the varistor sintered in  $890^\circ\text{C}$  was lower than the sample of  $870^\circ\text{C}$  slightly, this may be because the sintering reactions of raw materials did not begin or just started, but

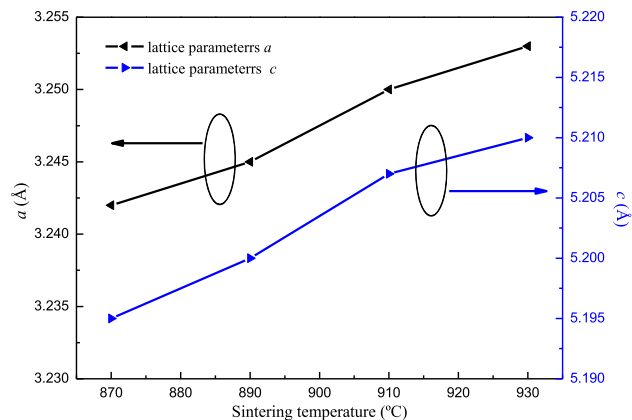


**Fig. 5** The lattice parameters of the varistors sintered in different temperatures

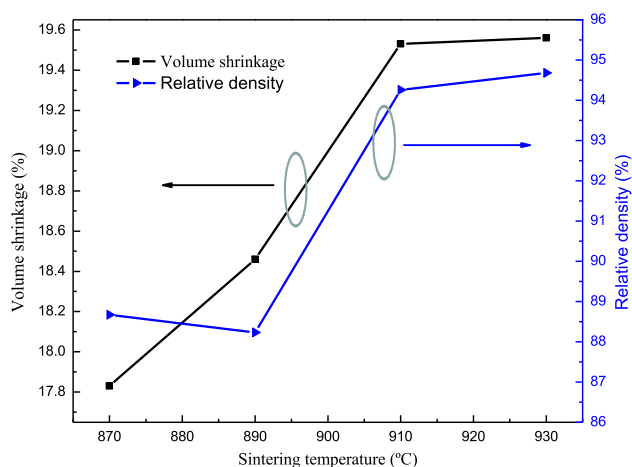


**Fig. 6** The relative density and volume shrinkage rate

meanwhile some low melting point materials, such as  $\text{Bi}_2\text{O}_3$  and  $\text{V}_2\text{O}_5$  had been volatilized.

### 3.2 Analysis of $E$ - $J$ characteristic

The electric field-current density ( $E$ - $J$ ) relation was shown in Fig. 7, and the value of nonlinear coefficient  $\alpha$ , breakdown electrical field  $E_{1\text{mA}}$  were shown in Table 1. It can be seen that the sintering temperature had significant influences on the  $E$ - $J$  characteristics such as breakdown electrical field  $E_{1\text{mA}}$  and nonlinear coefficient  $\alpha$ . The  $E_{1\text{mA}}$  decreased from  $5127.3$  to  $2687.5 \text{ V/cm}$  when the sintering temperature increased from  $870$  to  $930^\circ\text{C}$ . According to the Eq. (2), in which  $V_h$  is the varistor voltage of ZnO ceramic,  $V_g$  is the breakdown voltage of one barrier layer,  $D$  is the thickness of varistors,  $n$  is number of grain boundaries between the two electrodes, and  $d$  is the average grain size of ZnO, the value of  $E_{1\text{mA}}$  was inversely proportional to the value of average grain size  $d$ . So the value of  $E_{1\text{mA}}$  would decrease when the value of  $d$

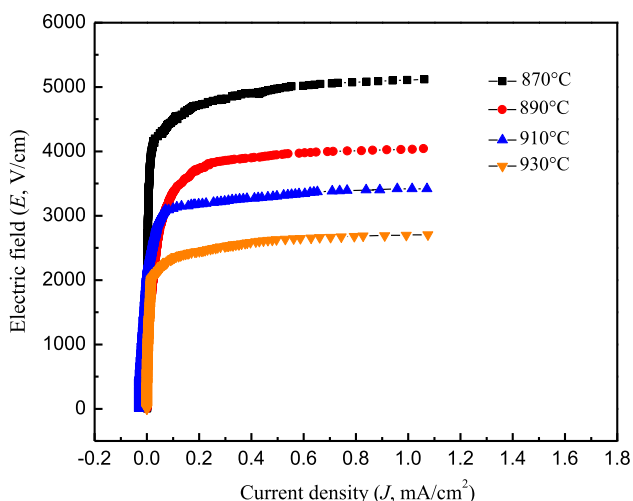


**Fig. 7** The  $E$ - $J$  characteristic of ZnO varistors sintered in different temperatures

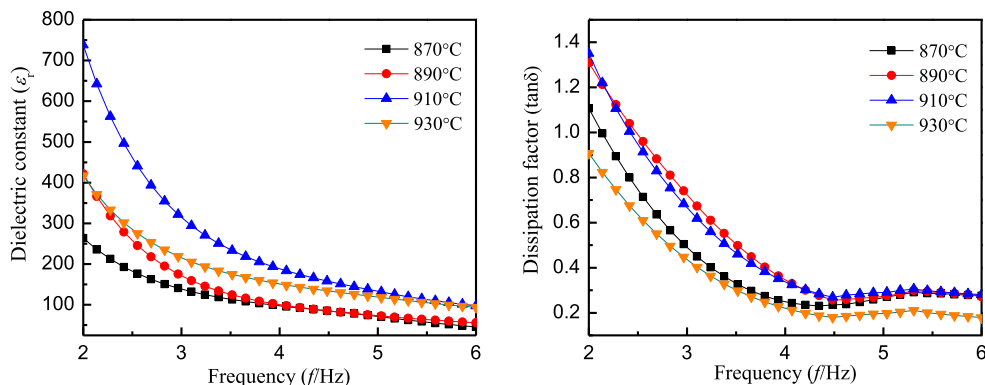
increased as the sintering temperature increasing. Meanwhile, the values of  $\alpha$  were 19.1, 23.3, 27.0 and 15.6, respectively when the sintering temperature increased from 870 to 930 °C. The value of  $\alpha$  was closely related with the content and distribution of grain boundary phases [26–29]. As the sintering temperature was 910 °C, the sintering reactions had begun. Meanwhile, there were a mass of grain boundary phases synthesized and they were distributed uniformly. So the ZnO varistors sintering at this temperature had a high value of  $\alpha$ .

$$V_h = nV_g = DV_g/d \tag{2}$$

### 3.3 Analysis of dielectric characteristic

The relative dielectric constant  $\epsilon_r$  and the dielectric loss  $\tan\delta$  changing with the frequency of ZnO varistors sintered in different temperatures were shown in Fig. 8. Both the values of  $\epsilon_r$  and  $\tan\delta$  decreased when the frequency increased, and the  $\tan\delta$  reached peak values when the frequency was 100 kHz. Meanwhile, when the frequency

**Fig. 8** The relative dielectric constant ( $\epsilon_r$ ) and the dielectric loss ( $\tan\delta$ ) changing with the frequency



was 10 kHz the values of  $\epsilon_r$  were 99.4, 103, 194, 154 and the values of  $\tan\delta$  were 0.26, 0.27, 0.29, 0.19 as the sintering temperature increasing, respectively, which all increased first and then decreased. When the frequency was 10 kHz, the relative dielectric constant  $\epsilon_r$  and the dielectric loss  $\tan\delta$  of ZnO varistors sintered in different temperatures changing with the test temperature were shown in Fig. 9. The results showed that the values of  $\epsilon_r$  and  $\tan\delta$  all increased first and then decreased when the test temperature increased. The  $\epsilon_r$  reached peak values when the test temperature was about 300 °C, and the  $\tan\delta$  reached peak values when it was about 275 °C. Meanwhile, the peak values of  $\epsilon_r$  and  $\tan\delta$  also increased first and then decreased when the sintering temperature increased.

### 3.4 Analysis of impedance and resistivity characteristic

When the test temperature was 175 °C, the Nyquist impedance charts of the ZnO varistors sintered in different temperatures were shown in Fig. 10, in which the  $z_r$  and  $z_i$  were the real part and imag part of the impedance respectively. The equivalent circuits of the samples could be simulated in Fig. 10. The number of branches of the circuits was determined by the number of grain boundaries, which was determined by the grain size and the uniformity of the microstructure. Combining with the result of SEM shown in Fig. 1, it can be found that the optimum sintering temperature should be 910 °C. On one hand, the microstructure of the ZnO varistor was more homogeneous and the grain size was between 1 and 1.5  $\mu\text{m}$ . On the other hand, the imag part of impedance of the grains was lower than the boundaries' in this sintering temperature (The left semicircle stands for the impedance of grains and the right one stands the impedance of boundaries). So the grains could be corresponded to components with high capacitance but low resistance, and the boundaries could be similar to units with high resistance but low capacitance, which would lead to the sensitivity to over voltages or currents [30–34].

**Fig. 9** The relative dielectric constant ( $\epsilon_r$ ) and the dielectric loss ( $\tan\delta$ ) changing with the test temperature

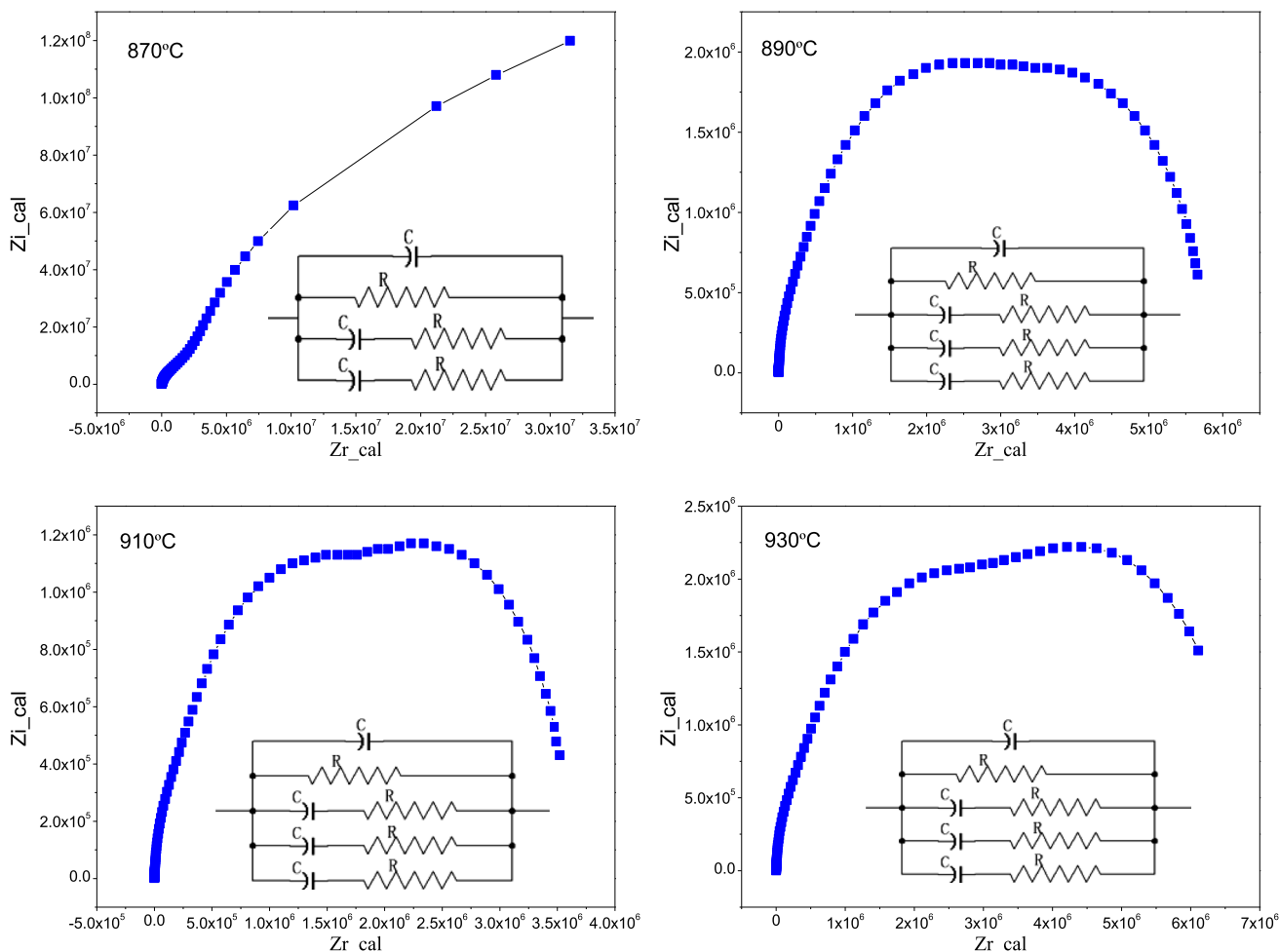
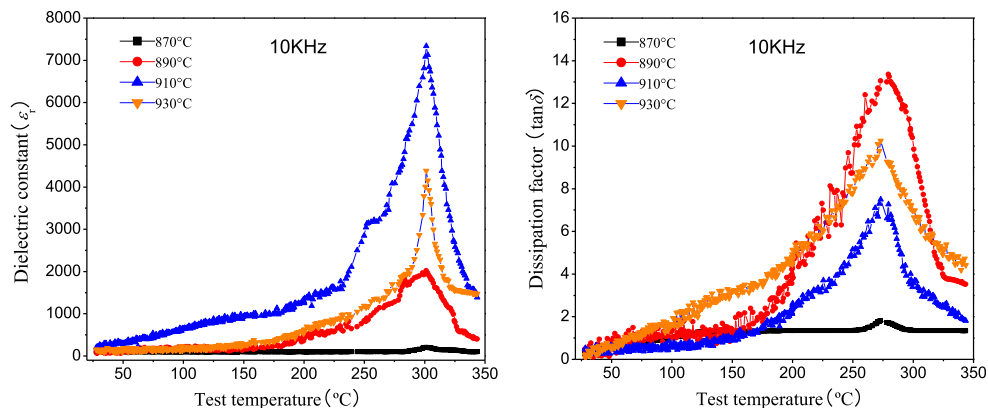


**Fig. 10** The Nyquist impedance atlas of the varistors at 175 °C

The relationship between the resistivity and the test temperature of the varistors sintered in different temperatures were indicated in Fig. 11. The results showed that all the varistors had high resistivity which ensured they would be stable and nearly insulative in the normal circuits [35, 36]. The resistivity of almost all the varistors had the maximum values when the test temperature was about

45 °C, then the resistivity decreased with the increase of test temperature. When the test temperature was above 175 °C, the resistivity values of all the samples would be the minimum but the most stable. Meanwhile, the resistivity of the varistor sintered at 910 °C had been very stable as the test temperature was below 100 °C and this value was about 1100 MΩ m. What's more, the

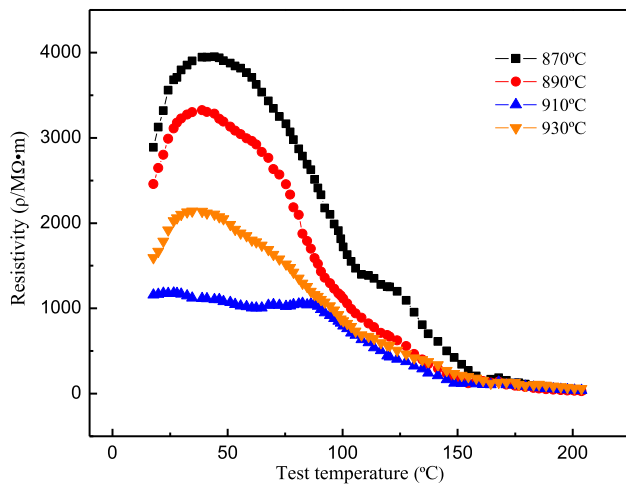


**Fig. 11** The relationship between the resistivity and the test temperature

temperature coefficient of resistance  $\alpha_T$  was only  $-0.67\%$  when the test temperature was between  $13.6$  and  $103.1\text{ }^\circ\text{C}$ , ensuring the stability and safety of the power electronic systems.

### 3.5 Comparison of different systems of varistors in some performances

The typical materials used for varistors mainly included ZnO and SnO<sub>2</sub>, and the ZnO varistors were used more and more widely in many areas. Zn–Bi and Zn–Pr were the main systems of ZnO varistors, however, it was reported that the Zn–Bi system varistors usually showed better performances due to the low sintering temperatures. Meanwhile, the Zn–Bi system varistors could be made into multilayer forms, which would improve their performances

significantly. In our work, the ZnO–Bi<sub>2</sub>O<sub>3</sub>–V<sub>2</sub>O<sub>5</sub> system varistor could be attributed to Zn–Bi system. Nevertheless, we had discussed more characteristics of Zn–Bi system varistor, such as microstructure,  $E$ – $J$  relation, dielectric, impedance and resistivity characteristics. The characteristics of ZnO varistor we discussed had been systematically compared with other reported varistors, and the results were summarized in Table 2. Obviously, the ZnO–Bi<sub>2</sub>O<sub>3</sub>–V<sub>2</sub>O<sub>5</sub> system varistor had a low sintering temperature and its  $E$ – $J$  characteristic was also comparable to or even more superior than others. Meanwhile, we had discussed the dielectric, impedance and resistivity characteristics of this varistor, it can be found that the varistor we studied had excellent dielectric characteristic, and the impedance and resistivity was also fairly stable. Therefore, the ZnO–Bi<sub>2</sub>O<sub>3</sub>–V<sub>2</sub>O<sub>5</sub> system varistor we studied here could be made into multilayer form, and its performance will be further improved. All the results reflected that the ZnO–Bi<sub>2</sub>O<sub>3</sub>–V<sub>2</sub>O<sub>5</sub> system varistor had greater application value, and the suitable sintering temperature we discussed could be  $910\text{ }^\circ\text{C}$ .

## 4 Conclusion

In this paper, the effects of sintering temperatures on the microstructure and electrical characteristics of the ZnO varistors were investigated systematically. When the sintering temperature increased from  $870$  to  $930\text{ }^\circ\text{C}$ , the average grain size enlarged from  $0.83$  to  $1.67\text{ }\mu\text{m}$ , the density increased from  $4.97$  to  $5.3\text{ g/cm}^3$  and the decrease of the breakdown electrical field  $E_{1mA}$  almost doubled. Meanwhile, the nonlinear coefficient  $\alpha$  showed a fluctuation phenomenon and the values of dielectric loss  $\tan\delta$

**Table 2** Comparison of different system of varistors in some characteristics

System of varistors	Main additives	Electrode material	Optimum sintering temperature ( $^\circ\text{C}$ )	Maximum value of $\alpha$	$E_{1mA}$ (V/cm)	Value of $\epsilon_r$	Value of $\tan\delta$	Value of $\alpha_T$	Stability of impedance	Refs.
ZnO–Bi <sub>2</sub> O <sub>3</sub> –V <sub>2</sub> O <sub>5</sub>	Bi <sub>2</sub> O <sub>3</sub> , V <sub>2</sub> O <sub>5</sub>	Pure silver	910	27.0	3456.5	194 (10 <sup>4</sup> Hz)	0.29 (10 <sup>4</sup> Hz)	$-0.67\%$	Fairly stable	This work
SnO <sub>2</sub> –Cr <sub>2</sub> O <sub>3</sub> –Sb <sub>2</sub> O <sub>3</sub>	Co <sub>3</sub> O <sub>4</sub>	Pure silver	1350	11.2	3218.3	–	–	–	Unstable	[23]
ZnO–Bi <sub>2</sub> O <sub>3</sub>	BN	Alloy silver	1000	43.3	3060.0	–	–	–	Unstable	[24]
ZnO–Bi <sub>2</sub> O <sub>3</sub>	Cr <sub>2</sub> O <sub>3</sub>	Pure silver	1000	80.7	3106.8	–	–	–	–	[27]
ZnO–Bi <sub>2</sub> O <sub>3</sub>	MnO <sub>2</sub>	Pure silver	930	50.2	2934.2	>1000 (10 <sup>4</sup> Hz)	Very high (10 <sup>4</sup> Hz)	–	–	[29]
ZnO–PrO <sub>1.83</sub>	Co <sub>2</sub> O <sub>3</sub>	Pure silver	1300	24.0	3471.0	–	–	–	Stable	[30]
ZnO–Bi <sub>2</sub> O <sub>3</sub>	Sb <sub>2</sub> O <sub>3</sub> , Co <sub>3</sub> O <sub>4</sub>	Pure silver	1200	2.8	200.0	–	–	–	–	[31]
ZnO–V <sub>2</sub> O <sub>5</sub>	MnO <sub>2</sub> , Nb <sub>2</sub> O <sub>5</sub>	Pure silver	900	19.5	4791.0	–	–	–	Stable	[32]
ZnO–PrO <sub>1.83</sub>	Er <sub>2</sub> O <sub>3</sub>	Pure silver	1100	29.0	1577.0	–	–	–	Stable	[33]
ZnO–Bi <sub>2</sub> O <sub>3</sub>	Zn powder	Silver	1190	56.7	3520.0	–	–	–	Unstable	[34]

were relatively high in this process. These phenomena had been explained in detail. The varistors sintering in 910 °C exhibited the excellent microstructure and uniformity as well as optimized electrical and dielectric characteristics, where  $\alpha$  was 27,  $E_{1mA}$  was 3456.5 V/cm; when the frequency was 10 kHz the values of  $\epsilon_r$  and  $\tan\delta$  were 194 and 0.29 at this sintering temperature, respectively; when the test temperature was between 13.6 and 103.1 °C, the value of  $\alpha_T$  was only  $-0.67\%$ , which was fairly stable at this sintering temperature.

**Acknowledgments** This work was supported by College of Electrical and Information Engineering, the School of Materials Science Engineering and the School of Science of Shaanxi University of Science and Technology. Meanwhile, it was supported by the National Natural Science Foundation of China (Grant No. 50972087) and the National Natural Science Foundation of China (Grant No. 51272145).

## References

- L.H. Cheng, L.Y. Zheng, Electrical properties of Al<sub>2</sub>O<sub>3</sub>-doped ZnO varistors prepared by sol-gel process for device miniaturization. *Ceram. Int.* **38S**, S457–S461 (2012)
- T.K. Gupta, Application of zinc oxide varistor. *Am. Ceram. Soc.* **73**, 1817–1840 (1990)
- M. Matsuoka, Nonohmic properties of zinc oxide ceramics. *J. Appl. Phys.* **10**, 736–740 (1971)
- C.W. Nahm, Low-temperature sintering effect on varistor properties of ZnO-V<sub>2</sub>O<sub>5</sub>-MnO<sub>2</sub>-Nb<sub>2</sub>O<sub>5</sub>-Bi<sub>2</sub>O<sub>3</sub> ceramics. *Ceram. Int.* **39**, 2117–2121 (2013)
- M.A. Ponce, M.A. Ramírez, Influence of degradation on the electrical conduction process in ZnO and SnO<sub>2</sub>-based varistors. *J. Appl. Phys.* **108**, 4505–4507 (2010)
- W. Mielcarek, A. Gubański, The effect of bismuth oxide polymorph forms on degradation processes in ZnO varistors. *Ceram. Int.* **39**, 8219–8226 (2013)
- C.W. Nahm, Characteristics of ZnO-V<sub>2</sub>O<sub>5</sub>-MnO<sub>2</sub>-Nb<sub>2</sub>O<sub>5</sub>-Er<sub>2</sub>O<sub>3</sub> semiconducting varistors with sintering processing. *Mater. Sci. Semicond. Process.* **16**, 778–785 (2013)
- H.H. Hing, K.Y. Tse, Grain growth of ZnO in binary ZnO-V<sub>2</sub>O<sub>5</sub> ceramics. *J. Mater. Sci.* **38**, 2367–2372 (2003)
- J.K. Tsai, T.B. Wu, Non-ohmic characteristics of ZnO-V<sub>2</sub>O<sub>5</sub> ceramics. *J. Appl. Phys.* **76**, 4817–4822 (1994)
- C.W. Nahm, Effect of sintering temperature on varistor properties and aging characteristics of ZnO-V<sub>2</sub>O<sub>5</sub>-MnO<sub>2</sub> ceramics. *Ceram. Int.* **35**, 2679–2683 (2009)
- H.K. Yong, H. Kawamura, M. Nawata, The effect of Cr<sub>2</sub>O<sub>3</sub> additive on the electrical properties of ZnO varistor. *J. Mater. Sci.* **32**, 1665–1670 (1997)
- J.F. Zhu, G.Q. Qi, Influence of intensive milling on the microstructure and electrical properties of ZnO-Bi<sub>2</sub>O<sub>3</sub>-based varistors. *Ceram. Int.* **38S**, S457–S461 (2012)
- K. Mukae, Electronic characterization of single grain boundary in ZnO prvaristors. *Ceram. Int.* **26**, 645–650 (2000)
- H. Jin, X. Xu, Reliability enhancement of zinc oxide varistors using sputtered silver electrodes. *Microelectron. Reliab.* **61**, 91–94 (2016)
- C. Salles, T.A. Nogueira, Effects of operation temperature in artificially aging of zinc oxide varistors by high current short impulses. *Electr. Power Syst. Res.* **134**, 145–151 (2016)
- D. Choron, S. Marinel, Construction of master sintering curves to understand the effect of Na addition on ZnO-based varistors. *J. Eur. Ceram. Soc.* **35**, 4195–4202 (2015)
- R. Rudez, J. Pavlic, Preparation and influence of highly concentrated screen-printing inks on the development and characteristics of thick-film varistors. *J. Eur. Ceram. Soc.* **35**, 3013–3023 (2015)
- M. Vukovic, G. Brankovic, Ultra-high breakdown field varistors prepared from individually synthesized nanoprecursors. *J. Eur. Ceram. Soc.* **35**, 1807–1814 (2015)
- T. Chen, M.H. Wang, Novel synthesis of monodisperse ZnO-based core/shell ceramic powders and applications in low-voltage varistors. *Mater. Des.* **96**, 329–334 (2016)
- Y. Beynet, A. Izoulet, ZnO-based varistors prepared by spark plasma sintering. *J. Eur. Ceram. Soc.* **35**, 1199–1208 (2015)
- E. Olsson, L.K. Falk, G.L. Dunlop, The microstructure of a ZnO varistor material. *J. Mater. Sci.* **20**, 4091–4098 (1985)
- P.L. Hower, T.K. Gupta, A barrier model for ZnO varistors. *J. Appl. Phys.* **50**, 4847–4855 (1979)
- J.A. Aguilar, P. Zambrano, Effect of high content of Co<sub>3</sub>O<sub>4</sub> on the structure, morphology, and electrical properties of (Cr, Sb)-doped SnO<sub>2</sub> varistors. *Ceram. Int.* **42**, 7576–7582 (2016)
- T. Chen, Q.Y. Fu, D.X. Zhou, Effects of BN on phase compositions and electrical properties of ZnO-Bi<sub>2</sub>O<sub>3</sub> varistors prepared by the reduction-reoxidation method. *J. Eur. Ceram. Soc.* **36**, 609–614 (2016)
- M.M. Oliveira, P.R. Bueno, Influence of La<sub>2</sub>O<sub>3</sub>, Pr<sub>2</sub>O<sub>3</sub> and CeO<sub>2</sub> on the nonlinear properties of SnO<sub>2</sub> multicomponent varistors. *Mater. Chem. Phys.* **74**, 150–153 (2002)
- C. Zang, Y.X. Hu, Influence of TiO<sub>2</sub>/Sb<sub>2</sub>O<sub>3</sub> ratio on ZnO varistor ceramics. *J. Eur. Ceram. Soc.* **22**, 61–65 (2002)
- H.R. Bai, S.H. Li, Influence of Cr<sub>2</sub>O<sub>3</sub> on highly nonlinear properties and low leakage current of ZnO-Bi<sub>2</sub>O<sub>3</sub> varistor ceramics. *Ceram. Int.* **42**, 10547–10550 (2016)
- K. Hembram, T.N. Rao, High performance varistors prepared from doped ZnO nanopowders made by pilot-scale flame spray pyrolyzer: sintering, microstructure and properties. *J. Eur. Ceram. Soc.* **35**, 3535–3544 (2015)
- Z.J. Xu, H.R. Bai, Effect of a Bi-Cr-O synthetic multi-phase on the microstructure and electrical properties of ZnO-Bi<sub>2</sub>O<sub>3</sub> varistor ceramics. *Ceram. Int.* **42**, 14350–14354 (2016)
- C.W. Nahm, Degradation behavior by DC-accelerated and pulse-current stress in Co/Cr/Y/Al/Ni co-doped ZnO-PrO<sub>1.83</sub>-based varistors. *Micro. Reliab.* **55**, 565–571 (2015)
- F. Kharchouche, E. Savary, Effects of microwave sintering on intrinsic defects concentrations in ZnO-based varistors. *Ceram. Int.* **40**, 13697–13701 (2014)
- C.W. Nahm, Aging characteristics of ZnO-V<sub>2</sub>O<sub>5</sub>-based varistors for surge protection reliability. *Micro. Reliab.* **54**, 2836–2842 (2014)
- C.W. Nahm, Aging characteristics of ZnO-PrO<sub>1.83</sub>-based semiconducting varistors for surge protection reliability. *Micro. Reliab.* **54**, 2417–2422 (2014)
- S.L. Jiang, Y.P. Wang, Effect of Zn doping on stability of ZnO varistors under high pulse-current stress. *Ceram. Int.* **41**, 11611–11617 (2015)
- M. Peiteado, A.M. Cruzb, Progressive degradation of high voltage ZnO commercial varistor sup on Fe<sub>2</sub>O<sub>3</sub> doping. *Ceram. Int.* **40**, 13395–13400 (2014)
- C.W. Nahm, Non-ohmic properties and impulse aging behavior of quaternary ZnO-V<sub>2</sub>O<sub>5</sub>-Mn<sub>3</sub>O<sub>4</sub>-Er<sub>2</sub>O<sub>3</sub> semiconducting varistors with sintering processing. *Mater. Sci. Semicond. Process.* **16**, 1308–1315 (2013)